JMEPEG (2012) 21:900–906
DOI: 10.1007/s11665-011-9970-8

1059-9495/$19.00

Effect of Thermal Oxidation on Corrosion Resistance of Commercially Pure Titanium in Acid Medium

M. Jamesh, Satendra Kumar, and T.S.N. Sankara Narayanan

(Submitted August 24, 2010; in revised form April 11, 2011)

This article addresses the characteristics of commercially pure titanium (CP-Ti) subjected to thermal oxidation in air at 650 °C for 48 h and its corrosion behavior in 0.1 and 4 M HCl and HNO_3 mediums. Thermal oxidation of CP-Ti leads to the formation of thick oxide scales (~20 μm) throughout its surface without any spallation. The oxide layer consists of rutile- and oxygen-diffused titanium as predominant phases with a hardness of 679 ± 43 $HV_{1.96}$. Electrochemical studies reveal that the thermally oxidized CP-Ti offers a better corrosion resistance than its untreated counterpart in both HCl and HNO_3 mediums. The uniform surface coverage and compactness of the oxide layer provide an effective barrier toward corrosion of CP-Ti. The study concludes that thermal oxidation is an effective approach to engineer the surface of CP-Ti so as to increase its corrosion resistance in HCl and HNO_3 mediums.

Keywords corrosion resistance, surface modification, thermal oxidation, titanium

1. Introduction

Titanium and its alloys have become the materials of choice in many industries due to their excellent corrosion resistance in a wide variety of environments (Ref 1). The formation of a thin self-adherent passive oxide film on their surface is considered responsible for this attribute. The corrosion rate of titanium and its alloys, however, is significant in hydrofluoric acid, caustic solutions, and uninhibited concentrated hydrochloric or sulfuric acid solutions that dissolve the protective oxide film or limit its formation. The increased use of titanium and its alloys in extractive metallurgy has prompted research into their corrosion behavior in various acids (Ref 2-9). Since the passive oxide film is responsible for the excellent corrosion resistance of titanium and its alloys, it is obvious that any treatment or modification that facilitates its formation and thickening would improve their corrosion performance. Addition of strongly oxidizing inorganic compounds such as $K_2Cr_2O_7$, $KMnO_4$, KIO_3, Na_2MoO_4, $NaClO_3$, Cl_2, and H_2O_2 tend to promote passivation of titanium. Addition of anions, such as iodate (IO_3^-), metavanadate (VO_3^-), and molybdate (MoO_4^{2-}) promoted passivation of Ti-6Al-4V alloy in 2.5 M H_2SO_4 and 5.0 M HCl (Ref 5). Tomashov et al. (Ref 10, 11) have shown that the greatest increase in corrosion resistance occurs when titanium is alloyed with palladium and other noble metals, which are capable of shifting the corrosion potential in the noble direction. Alloying of titanium with molybdenum, chromium, aluminum, zirconium, and tantalum, which increases its tendency to passivate, also enables a beneficial influence (Ref 10-14).

Surface modification is a promising way to increase the surface hardness, corrosion resistance, and wear resistance of titanium and its alloys. Numerous surface modification methods, such as chemical treatment (acid and alkali treatment) (Ref 15, 16), electrochemical treatment (anodic oxidation) (Ref 17), chemical vapor deposition (Ref 18), physical vapor deposition (Ref 19), sol-gel coatings (Ref 20), plasma spray deposition (Ref 21), ion implantation (Ref 22), thermal oxidation (Ref 23), etc., have been explored. Among these methods, thermal oxidation is considered as a cost-effective method to deliberately generate a barrier oxide layer of relatively higher thickness (~20-30 μm) on titanium compared to the naturally formed oxide layer (typically of 4-6 nm). Thermal oxidation of titanium is aimed to produce in situ ceramic coatings, mainly based on rutile, in the form of a thick, highly crystalline oxide film, which is accompanied by the dissolution of oxygen beneath them. The thermally formed oxide layer enables an increase in hardness, wear resistance, and corrosion resistance of titanium and its alloys (Ref 24-31). The ability of thermally oxidized (TO) commercially pure titanium (CP-Ti) and Ti-6Al-4V alloy in improving the corrosion and fretting corrosion resistance in Ringer's solution has been reported in our earlier articles (Ref 29-33). This article aims to evaluate the corrosion behavior of the TO CP-Ti in HCl and HNO_3 (0.1 and 4 M) by open circuit potential (OCP)-time measurement and potentiodynamic polarization studies for industrial application.

2. Experimental Details

The CP-Ti (Grade 2, chemical composition in wt.%: N, 0.01; C, 0.03; H, 0.01; Fe, 0.20; O, 0.18; and Ti: Balance) having a dimension of $3 \times 4 \times 0.2$ cm^3 was used as the substrate material. Before thermal oxidation, the CP-Ti samples were abraded using successive grit size of SiC-coated abrasive papers (60, 100, 220, 320, 400, 600, 800, and 1000 μm,

M. Jamesh, Satendra Kumar, and **T.S.N. Sankara Narayanan**, National Metallurgical Laboratory, Madras Centre, CSIR Madras Complex, Taramani, Chennai 600 113, India. Contact e-mail: tsnsn@rediffmail.com.

respectively), followed by thorough rinsing with deionized water and acetone. Thermal oxidation of CP-Ti samples was performed using a muffle furnace in air at 650 °C for 48 h. The CP-Ti was placed inside the furnace, and the temperature was increased at a heating rate of 5 °C/min (the thermal treatment includes ramping step). Once it reached 650 °C, the CP-Ti samples were soaked at this temperature for 48 h (this 48 h does not include any ramping step). After thermal oxidation, the samples were allowed to cool in the furnace itself, at its natural cooling rate. The phase constituents of the untreated and the TO CP-Ti samples, and the nature of the oxide film formed on the surface were determined by x-ray diffraction (D8 DISCOVER, Brucker axs) using Cu-Kα radiation. The thickness of the oxide layer was determined using scanning electron microscopy (SEM). For measuring the thickness of the thermally oxidized layer, the cross section of the treated sample was analyzed using scanning electron microscopy. The TO CP-Ti sample was cut using a slow speed cutter (Buehler) using a very low load, followed by mounting, abrading using various grit size SiC-coated abrasive papers and polishing applying 0.3 μm alumina paste to obtain a mirror finish. The polished samples were thoroughly rinsed with deionized and etched with Kroll's reagent (HNO_3: 6 mL; HF: 2 mL; and Deionized water: 92 mL), a well-known etching agent for titanium and its alloys, for 10-15 s. Surface morphology of the oxide layer was assessed by SEM. The microhardness of the untreated and TO CP-Ti samples was measured at the surface using a Leica Vickers microhardness tester at a load of 1.96 N applied for 15 s. Seven indentations were made on each sample, and the values were averaged out. The corrosion behavior of the untreated and TO CP-Ti samples in HCl and HNO_3 (0.1 and 4 M) was evaluated by OCP-time measurements and potentiodynamic polarization studies using a potentiostat/galvanostat/frequency response analyzer of ACM instruments (Model: Gill AC). The untreated and TO CP-Ti samples form the working electrodes, while a saturated calomel electrode (SCE) and graphite rod were used as the reference and auxiliary electrodes, respectively. These electrodes were placed within a flat cell in such a way that only 1 cm^2 area of the working electrode was exposed to the electrolyte solution. The HCl and HNO_3 (0.1 and 4 M) solutions were kept open to air and they were maintained at 27 ± 1 °C. Before performing the potentiodynamic polarization studies, the untreated and TO CP-Ti samples were allowed to stabilize in HCl and HNO_3 (0.1 and 4 M) for 30 min. during which the change in OCP was recorded as a function of time. Potentiodynamic polarization measurements were carried out in the potential range from −250 to +3000 mV relative to OCP versus SCE at a scan rate of 100 mV/min. The scan rate used for polarization study is an important parameter and if not chosen properly it would incorrectly reflect the corrosion process. During the corrosion process, the electrode surface can be considered as a simple resistor (solution resistance) in series with a parallel combination of a resistor (polarization resistance) and capacitor (double layer capacitance). Hence, the scan rate should be slow enough so that the capacitors remain fully charged and the current/voltage relationship reflects only the interfacial corrosion process at every potential of the polarization scan. Otherwise, it would reflect charging of the surface capacitance in addition to the corrosion process. In such conditions, the measured current would be greater than the current actually generated by the corrosion reactions. The estimated maximum scan rates for several combinations of polarization resistances, solution resistances, and capacitances, which are often encountered in practice is complied by Silverman (Ref 34). Accordingly, for a combination of solution resistance, charge transfer/film resistance and capacitance of 10 Ω cm^2, 10^3-10^4 Ω cm^2, and 100 μF, the recommended scan rate lies between 0.51 and 5.1 mV/s. In this study, a scan rate of 100 mV/min. (i.e., 1.67 mV/s.) is used. Moreover, while choosing the scan rate for polarization study, one should maintain an appropriate balance between the slow scan rates and quickly get the required information. In addition, the scan rates should be kept similar to ensure consistent comparison between the untreated and the treated samples in a given environment. A scan rate of 100 mV/min. has been used in previous studies (Ref 29-31, 35) the authors of this study as well as by other researchers (Ref 36, 37). The very high potential (up to +3000 mV) is employed to study the passivation behavior. The corrosion potential (E_{corr}) and corrosion current density (i_{corr}) were determined from the polarization curves using Tafel extrapolation method. To compare the passivation ability of the untreated and TO CP-Ti, the passive current density (i_{pass}) is determined at +850 mV versus SCE. The choice of this potential was made on the basis that it should be on the passive region, and it should not face any interference from oxygen evolution. The potentiodynamic polarization studies were repeated at least three times to ensure reproducibility of the test results. Since the pattern/trend of the polarization curves do not exhibit any variation between the triplicate measurements, only one curve was selected as a representative curve for subsequent analysis.

3. Results and Discussion

3.1 Characteristics of Thermally Oxidized CP-Ti

The surface morphology of the TO CP-Ti (at 650 °C for 48 h) reveals the presence of oxide scales throughout the surface without any spallation (Fig. 1a). The oxide scales, however, are relatively rougher. The mechanism of thermal oxidation of CP-Ti has already been described in our earlier articles (Ref 29, 31). Accordingly, nucleation of oxide takes place throughout the surface when it immediately encounters oxygen whereas the growth mode involves the formation of a thin oxide scale followed by its agglomeration and growth, completely covering the surface. Hence, when the CP-Ti sample is oxidized at 650 °C for 48 h, one would expect a considerable grain growth during which each oxide grain is attached with its neighboring grains to enable the formation of a thick and homogeneous oxide layer. The cross-sectional view of the oxidized the CP-Ti sample confirms this phenomenon (Fig. 1b). The XRD patterns of the untreated and TO CP-Ti are shown in Fig. 2. The untreated CP-Ti is entirely composed of hexagonal α-phase (denoted as "Ti" in Fig. 2). The XRD pattern of the TO CP-Ti exhibits the presence of rutile (denoted as "R" in Fig. 2) and oxygen-diffused Ti (TiO) as the predominant phases. The predominance of peaks pertaining to rutile with a corresponding decrease in the intensity of the peaks pertaining to α-Ti confirms the formation of a thick (~20-25 μm) and homogeneous oxide layer (Fig. 1b), which would otherwise exhibit α-Ti as the predominant peak in the XRD pattern. The formation of rutile- and oxygen-diffused Ti (TiO) was observed earlier by other researchers (Ref 23, 24, 27, 38). Siva Rama Krishna et al. (Ref 27) have reported the

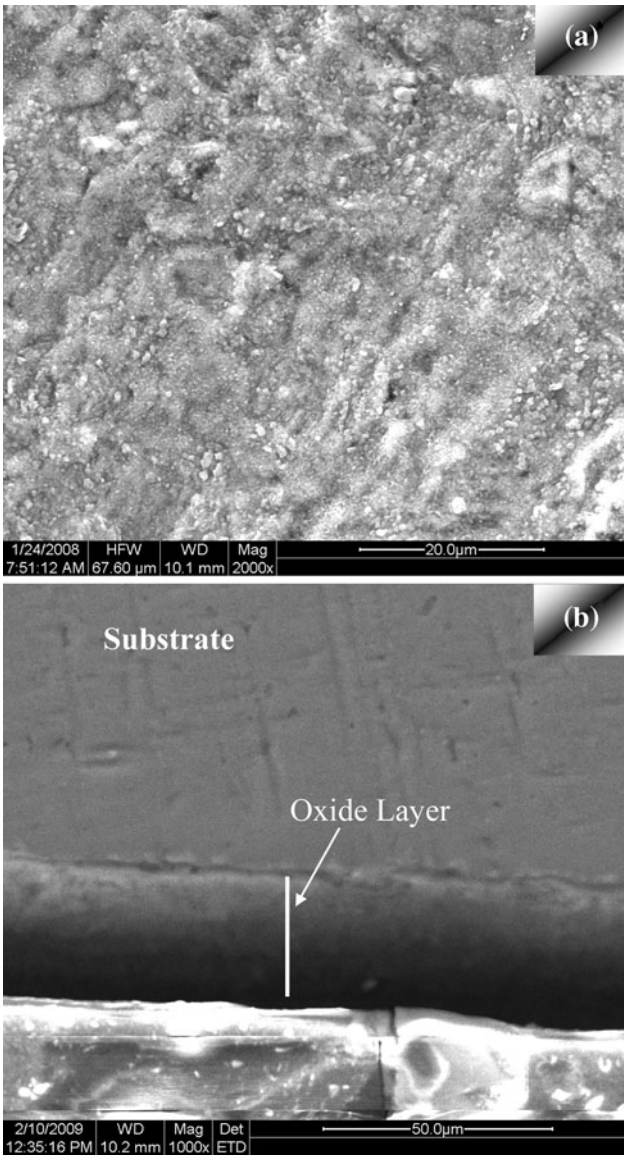

Fig. 1 Surface morphology (a) and cross-sectional view (b) of CP-Ti thermally oxidized in air at 650 °C for 48 h

formation of TiO at temperatures less than 700 °C and rutile at and above 800 °C as dominant phases following oxidation of titanium. Guleryuz and Cimenoglu (Ref 23, 38) have reported the presence of anatase phase for samples oxidized at 600 °C for 24 and 48 h whereas rutile was the only dominated phase when the samples were oxidized at 650 °C for 48 h. In this study, no anatase phase is found when the CP-Ti sample is subjected to thermal oxidation in air at 650 °C for 48 h. Thermal oxidation of CP-Ti enables a significant improvement in surface hardness due to the formation of a hard oxide layer and the presence of an oxygen diffusion zone beneath it. Almost a three-fold increase in hardness from 178 ± 6 to 679 ± 43 $HV_{1.96}$ is observed for CP-Ti after thermal oxidation at 650 °C for 48 h. With such an improvement in hardness, one would expect an improvement in wear resistance for TO CP-Ti. It has been reported that the mechanical properties of Ti and its alloys are influenced by the experimental conditions used for TO, such as treatment temperature, time and air/furnace cooling (Ref 27, 31, 39-42). Increase in treatment temperature during

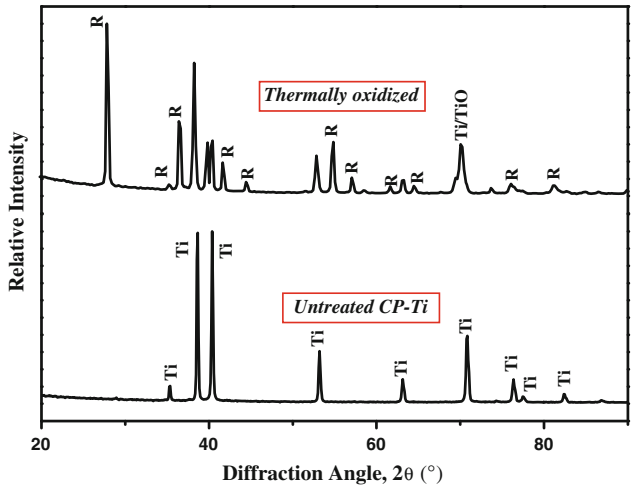

Fig. 2 XRD patterns of untreated and thermally oxidized (650 °C/48 h) CP-Ti

TO of CP-Ti increased the hardness and roughness (Ref 31). A sixfold increase in hardness is observed when the CP-Ti samples oxidized at 800 °C for 48 h compared to that of the untreated CP-Ti. Ebrahimi et al. (Ref 39) have reported that increase in treatment time increased the surface hardness and hardening depth for thermally oxidized Ti-4Al-2V alloy. According to Siva Rama Krishna et al. (Ref 27), when the oxide layer formed on the CP-Ti is subjected to cooling in furnace than in air, then, it would possess low porosity, higher hardness with less deviation in hardness, good adhesive strength, and excellent friction characteristics and wear resistance. Ebrahimi et al. (Ref 39) have reported that the fatigue limit of Ti-4Al-2V alloy is slightly improved when it is oxidized at 600 °C compared to its untreated counterpart. However, when the alloy is oxidized at 750 °C, a significant decrease in the fatigue limit is observed. Leinenbach and Eifler (Ref 42) have reported that the TO of CP-Ti at 570 °C for 3 h followed by air cooling leads to a poor fatigue limit. According to them, cooling of the thermally oxidized samples in air or furnace would significantly affect the mechanical properties of the TO CP-Ti. If the oxide layer is compact with one narrow homogeneous diffusive zone and the oxygen content of the surface layer is increased, then an improvement in fatigue limit is expected. In contrast, compressive residual stress and crystalline nature of the oxide layer would decrease the fatigue limit (Ref 39-42). In this study, the CP-Ti samples were subjected to thermal oxidation at 650 °C for 48 h followed by furnace cooling at its natural cooling rate. The resultant oxide layer is uniform, compact, adherent and possesses a higher hardness. Hence, it is not expected to cause a significant decrease in the fatigue limit of CP-Ti.

3.2 Corrosion Behavior of Untreated and Thermally Oxidized CP-Ti

The OCP-time curves of the untreated and TO CP-Ti in HCl and HNO_3 medium (0.1 and 4 M) are shown in Fig. 3. There is no appreciable change in OCP for the untreated CP-Ti in both 0.1 and 4 M HCl while some fluctuations are observed for the TO CP-Ti in 0.1 and 4 M HCl. Yu et al. (Ref 43) have observed an abrupt decrease in OCP due to thinning of the naturally formed passive oxide layer followed by uniform dissolution

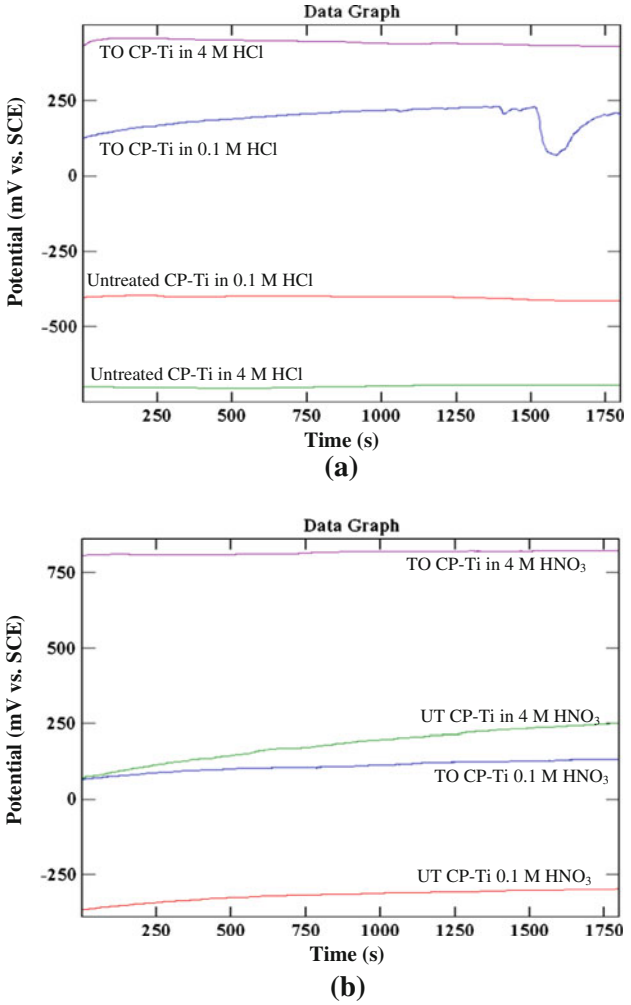

Fig. 3 Open circuit potential (OCP)-time curves of untreated and TO CP-Ti in 0.1 and 4 M in (a) HCl and (b) HNO_3 mediums

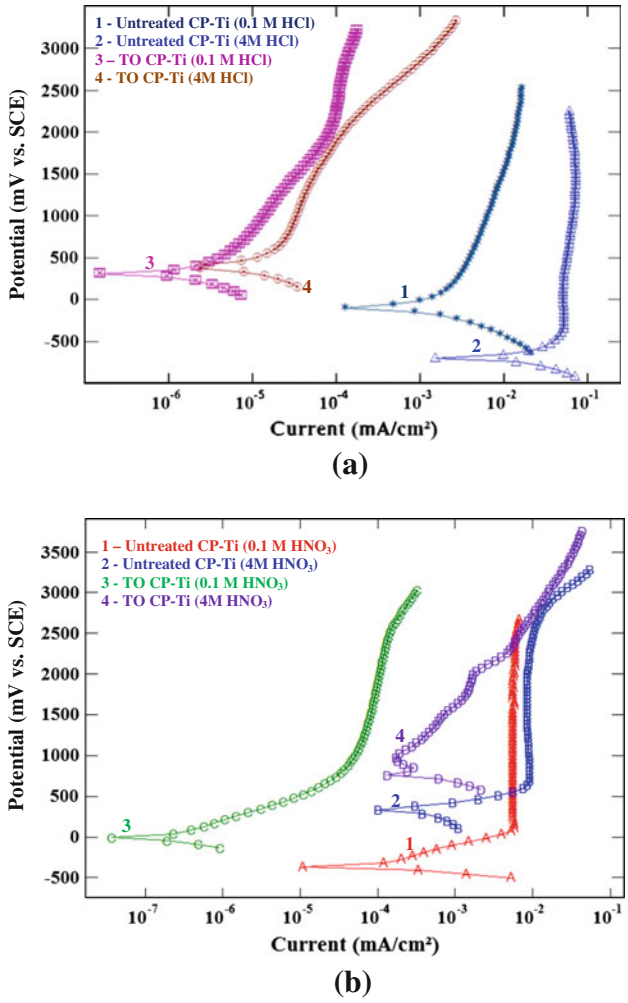

Fig. 4 Potentiodynamic polarization curves of untreated and TO CP-Ti in (a) HCl and (b) HNO_3 medium

and subsequent surface activation of Ti-45Nb and Ti-50Zr alloys in 5 M HCl at 37 °C. However, they have noticed a positive shift in OCP at 1 M HCl (Ref 43). The dependence of HCl concentration on the corrosion behavior and the difficulty in thickening of the air formed passive oxide layer at higher concentrations of HCl are also observed in this study. In HNO_3 medium, an anodic shift in OCP is observed at both concentrations, with the effect being well pronounced at 4 M. This is due to the oxidizing nature of HNO_3, which promotes passivation and helps to increase the thickness of the passive layer. A similar attribute has been made by Robin et al. (Ref 2) for Ti-4Al-4V alloy in HNO_3 medium. The dependence of increase in thickness with the concentration of HNO_3 further supports this view. The extent of anodic shift in OCP is relatively less for the TO CP-Ti than the untreated one. The OCP of both the untreated and TO CP-Ti in HNO_3 mediums are in the TiO_2 stability region of the Ti-H_2O Pourbaix diagram (Ref 44).

The potentiodynamic polarization curves of the untreated and TO CP-Ti in HCl and HNO_3 are presented in Fig. 4(a) and (b), respectively. The untreated CP-Ti samples exhibit passivity in the anodic region of the polarization curve in both HCl and HNO_3 mediums (0.1 and 4 M). During polarization, untreated CP-Ti samples translate directly from "Tafel region" into a stable passive state, without exhibiting any active-passive transition. The TO CP-Ti samples exhibit an active-passive transition only in 4 M HNO_3 whereas a direct transition from "Tafel region" into a passive state without any active-passive transition is observed in 0.1 M HNO_3 as well as in 0.1 and 4 M HCl (Ref 45-47). The passive current density (i_{pass}) is stable even up to +2000 mV versus SCE for the untreated CP-Ti whereas a continuous increase in i_{pass} with increase in potential is observed for TO CP-Ti. The i_{pass} of both the untreated and TO CP-Ti are higher than their respective corrosion current densities (i_{corr}). A similar observation is also made earlier by many researchers (Ref 47-50). Nevertheless, the i_{pass} of TO CP-Ti, measured at +850 mV versus SCE is relatively lower than that of the untreated CP-Ti. In general, materials that show a positive shift in corrosion potential (E_{corr}) and a decrease in i_{corr} offer a better corrosion resistance and vice-versa (Ref 29-31, 35). In this study, a significant positive shift in E_{corr} and a substantial decrease in i_{corr} are observed for the TO CP-Ti than for the untreated CP-Ti in both HCl and HNO_3 mediums (0.1 and 4 M), which clearly suggest the ability of the TO CP-Ti samples to offer a better corrosion resistance. The E_{corr}, i_{corr}, and i_{pass} of the untreated and TO CP-Ti are compiled in Table 1. In 4 M HNO_3, the E_{corr} of both the untreated and TO CP-Ti is shifted toward nobler direction when compared to their

Table 1 Corrosion potential (E_{corr}), corrosion current density (i_{corr}), and passive current density (i_{pass}) of untreated and TO CP-Ti in HCl and HNO_3 mediums (0.1 and 4 M) calculated from potentiodynamic polarization studies

Type of sample tested	Electrolyte used	E_{corr}, mV vs. SCE	i_{corr}, μA/cm^2	i_{pass}(a), μA/cm^2
Untreated CP-Ti	0.1 M HCl	−412	0.63	5.5
	4 M HCl	−703	27.00	63.7
TO CP-Ti	0.1 M HCl	+173	0.0009	0.008
	4 M HCl	+239	0.0077	0.03(b)
Untreated CP-Ti	0.1 M HNO_3	−369	0.047	5.6
	4 M HNO_3	+330	0.23	9.2
TO CP-Ti	0.1 M HNO_3	−6	0.0001	0.04
	4 M HNO_3	+761	0.075	0.3(b)

(a) Measured at +850 mV vs. SCE. (b) Continuous increase in i_{pass}

OCP. This clearly shows the ease of passivation of both the untreated and TO CP-Ti in 4 M HNO_3 following the strong oxidizing nature of HNO_3.

Potentiodynamic polarization studies reveal that the TO CP-Ti offers a better corrosion resistance than the untreated CP-Ti in both HCl and HNO_3 mediums (Fig. 4; Table 1). The improvement in corrosion resistance is believed to be due to the coverage of its surface by thicker oxide (∼20 μm) scale, which serves as an effective barrier layer, physically separating it from the acid medium. Since the oxide layer formed on the CP-Ti is allowed to cool in the furnace than in air, it would possess a lower porosity (Ref 27). If it were a porous layer, then it would not be possible to observe lower i_{corr} values from polarization studies. It has been reported in the literature that the experimental conditions used for thermal oxidation might result with either an effective barrier layer or porous layer (Ref 27, 39, 51). Thermal oxidation on Ti and Ni-Ti alloys, and their characterization by impedance was studied by Barisona et al. (Ref 52). The TO film on Ni-Ti alloy consists of outer porous layer due to the presence of Ni and inner compact layer having nickel free TiO_2 rutile. However, TO Ti sample consists of single compact layer. Several researchers have also confirmed the ability of TO CP-Ti and Ti-6Al-4V alloy to offer a better corrosion resistance in a variety of environments (Ref 23, 28-33, 38). Guleryuz and Cimenoglu (Ref 23) have reported that Ti-6Al-4V alloy subjected to thermal oxidation in air at 600 °C offered an excellent corrosion resistance than its untreated counterpart when they are subjected to accelerated corrosion test in 5 M HCl. According to those authors, no loss in weight is observed for thermally oxidized Ti-6Al-4V alloy even after 36 h of immersion due to the formation of a thick and stable oxide film on the surface of the Ti-6Al-4V alloy. Bloyce et al. (Ref 28) have compared the corrosion resistance of untreated, plasma nitrided (PN), thermally oxidized (TO), palladium-treated thermally oxidized (PTO) CP-Ti in 3.5% NaCl solution at room temperature by potentiodynamic polarization studies. Both TO and PTO CP-Ti samples exhibit a shift in E_{corr} toward the noble direction and a decrease in i_{corr} compared to that of PN and untreated CP-Ti. They have also evaluated the corrosion resistance of these samples by the accelerated corrosion test that involves immersion in boiling 20% HCl. Both TO and PTO CP-Ti samples increased the lifetime by a factor of about 13 and 27, respectively, when compared to that of PN CP-Ti. The results of this study further confirm the fact that thermal oxidation would lead to the formation of an effective barrier layer on CP-Ti and offer an excellent corrosion resistance compared to the untreated CP-Ti in both HCl and HNO_3 mediums at both 0.1 and 4 M concentrations.

4. Conclusion

Thermal oxidation of CP-Ti in air at 650 °C for 48 h leads to the formation of thick oxide scales (∼20 μm) throughout the surface without any spallation. The oxide layer consists of rutile- and oxygen-diffused Ti as the predominant phases. The hard oxide layer on the surface and the presence of an oxygen diffusion zone beneath it enable a significant improvement in the hardness from 178 ± 6 to 679 ± 43 $HV_{1.96}$. No appreciable change in OCP with time is observed for both the untreated and TO CP-Ti in HCl mediums, whereas an anodic shift in OCP as a function of time is observed in HNO_3 medium at both concentrations (0.1 and 4 M) with the effect being well pronounced at 4 M. The oxidizing nature of HNO_3 promotes passivation and helps to increase the thickness of the passive layer. Compared to the untreated one, the polarization curves of the TO CP-Ti are shifted toward lower current region in both HCl and HNO_3 medium. Potentiodynamic polarization studies reveal that the TO CP-Ti offers a better corrosion resistance than the untreated CP-Ti in both HCl and HNO_3 mediums. The improvement in corrosion resistance is due to the coverage of its surface by thicker oxide (∼20 μm) scale, which serves as an effective barrier layer, physically separating it from the acid medium. The study concludes that thermal oxidation offers an effective means of engineering the surface to increase the corrosion resistance of the CP-Ti in HCl and HNO_3 mediums.

Acknowledgment

The authors express their sincere thanks to Dr. S. Srikanth, Director, National Metallurgical Laboratory, Jamshedpur, for his constant support and encouragement to carry out this research study and permitting publication of this article.

References

1. B.D. Craig and D.S. Anderson, *Handbook of Corrosion Data*, ASM International, Materials Park, OH, 1995
2. A. Robin, J.L. Rosa, and H.R.Z. Sandim, Corrosion Behavior of Ti-4Al-4V Alloy in Nitric, Phosphoric and Sulphuric Acid Solutions at Room Temperature, *J. Appl. Electrochem.*, 2001, **31**, p 455–460

3. D.J. Blackwood and S.K.M. Chooi, Stability of Protective Oxide Films Formed on a Porous Titanium, *Corros. Sci.*, 2002, **44**, p 395–405
4. A.S. Mogoda, Y.H. Ahmad, and W.A. Badawy, Corrosion Behaviour of Ti-6Al-4V Alloy in Concentrated Hydrochloric and Sulphuric Acids, *J. Appl. Electrochem.*, 2004, **34**, p 873–878
5. A.S. Mogoda, Y.H. Ahmad, and W.A. Badawy, Corrosion Inhibition of Ti-6Al-4V Alloy in Sulfuric and Hydrochloric Acid Solutions Using Inorganic Passivators, *Mater. Corros.*, 2004, **55**, p 449–456
6. M.V. Popa, E. Vasilescu, P. Drob, C. Vasilescu, J. Mirza-Rosca, and A. Santana Lopez, Corrosion Behavior of Some Titanium Base Alloys in Acid Solutions, *Mater. Manuf. Process.*, 2005, **20**, p 35–45
7. J. Vaughan and A. Alfantazi, Corrosion of Titanium and Its Alloys in Sulfuric Acid in the Presence of Chlorides, *J. Electrochem. Soc.*, 2006, **153**, p B6–B12
8. K. Azumi, M. Nakajima, K. Okamoto, and M. Seo, Dissolution of Ti Wires in Sulphuric Acid and Hydrochloric Acid Solutions, *Corros. Sci.*, 2007, **49**, p 469–480
9. R.Sh. Razavi, M. Salehi, M. Ramazani, and H.C. Man, Corrosion Behaviour of Laser Gas Nitrided Ti-6Al-4V in HCl Solution, *Corros. Sci.*, 2009, **51**, p 2324–2329
10. N.D. Tomashov, R.M. Altovsky, and G.P. Chernova, Passivity and Corrosion Resistance of Titanium and its Alloys, *J. Electrochem. Soc.*, 1961, **108**, p 113–119
11. N.D. Tomashov, G.P. Chernova, Yu.S. Ruscol, and G.A. Ayuyan, The Passivation of Alloys on Titanium Bases, *Electrochim. Acta*, 1974, **19**, p 159–172
12. S. Piazza, G. Lo Biundo, N.C. Romano, C. Sunseri, and F. di Quatro, In Situ Characterization of Passive Films on Al-Ti Alloy by Photocurrent and Impedance Spectroscopy, *Corros. Sci.*, 1998, **40**, p 1087–1108
13. C.M. Chen, F.H. Beck, and M.G. Fontana, Stress Corrosion Cracking of Ti-8Al-1Mo-1V Alloy, *Corrosion*, 1970, **26**, p 135–139
14. K. Azumi, S. Watanabe, M. Seo, I. Saecki, Y. Inokuchi, P. James, and W.N. Smyrl, Characterization of Anodic Oxide Film Formed on Tin Coating in Neutral Borate Buffer Solution, *Corros. Sci.*, 1998, **40**, p 1363–1377
15. C. Sittig, M. Textor, N.D. Spencer, M. Wieland, and P.H. Vallotton, Surface Characterization of Implant Materials CP-Ti, Ti-6Al-7Nb and Ti-6Al-4V with Different Pretreatments, *J. Mater. Sci. Mater. Med.*, 1999, **10**, p 35–46
16. H.B. Wen, J.G. Wolke, J.R. Wijn, Q. Liu, F.Z. Cui, and K. de Groot, Fast Precipitation of Calcium Phosphate Layers on Titanium Induced by Simple Chemical Treatments, *Biomaterials*, 1997, **18**, p 1471–1478
17. X. Nie, E.I. Meletis, J.C. Jiang, A. Leyland, A.L. Yerokhin, and A. Matthews, Abrasive Wear/Corrosion Properties and TEM Analysis of Al_2O_3 Coatings Fabricated Using Plasma Electrolysis, *Surf. Coat. Technol.*, 2002, **149**, p 245–251
18. P. Andreazza, M.I. De Barros, C. Andreazza-Vignolle, D. Rats, and L. Vandenbulcke, In-Depth Structural X-ray Investigation of PECVD Grown Diamond Films on Titanium Alloys, *Thin Solid Films*, 1998, **319**, p 62–66
19. M. Uchida, N. Nihira, A. Mitsuo, K. Toyoda, K. Kubota, and T. Aizawa, Friction and Wear Properties of CrAlN and CrVN Films Deposited by Cathodic Arc Ion Plating Method, *Surf. Coat. Technol.*, 2004, **177–178**, p 627–630
20. T. Brendel, A. Engel, and C. Russel, Hydroxyapatite Coatings by a Polymeric Route, *J. Mater. Sci. Mater. Med.*, 1992, **3**, p 175–179
21. S.W.K. Kweh, K.A. Khor, and P. Cheang, An In Vitro Investigation of Plasma Sprayed Hydroxyapatite (HA) Coatings Produced with Flame-Spheroidized Feedstock, *Biomaterials*, 2002, **23**, p 775–785
22. T. Hanawa, Y. Kamiura, S. Yamamoto, T. Kohgo, A. Amemiya, H. Ukai et al., Early Bone Formation Around Calcium-Ion-Implanted Titanium Inserted into Rat Tibia, *J. Biomed. Mater. Res.*, 1997, **36**, p 131–136
23. H. Guleryuz and H. Cimenoglu, Effect of Thermal Oxidation on Corrosion and Corrosion-Wear Behaviour of a Ti-6Al-4V Alloy, *Biomaterials*, 2004, **25**, p 3325–3333
24. M.F. Lopez, J.A. Jimenez, and A. Gutierrez, Corrosion Study of Surface-Modified Vanadium-Free Titanium Alloys, *Electrochim. Acta*, 2003, **48**, p 1395–1401
25. D. Velten, V. Biehl, F. Aubertin, B. Valeske, W. Possart, and J. Breme, Preparation of TiO(2) Layers on CP-Ti and Ti6Al4V by Thermal and Anodic Oxidation and by Sol-Gel Coating Techniques and Their Characterization, *J. Biomed. Mater. Res.*, 2002, **59**, p 18–28
26. M.L. Escudero, J.L. Gonzalez-Carrasco, C. Garcia-Alonso, and E. Ramirez, Electrochemical Impedance Spectroscopy of Preoxidized MA 956 Superalloy During In Vitro Experiments, *Biomaterials*, 1995, **16**, p 735–740
27. D. Siva Rama Krishna, Y.L. Brama, and Y. Sun, Thick Rutile Layer on Titanium for Tribological Applications, *Tribol. Int.*, 2007, **40**, p 329–334
28. A. Bloyce, P.Y. Qi, H. Dong, and T. Bell, Surface Modification of Titanium Alloys for Combined Improvements in Corrosion and Wear Resistance, *Surf. Coat. Technol.*, 1998, **107**, p 125–132
29. S. Kumar, T.S.N. Sankara Narayanan, S. Ganesh Sundara Raman, and S.K. Seshadri, Thermal Oxidation of CP-Ti: Evaluation of Characteristics and Corrosion Resistance as a Function of Treatment Time, *Mater. Sci. Eng. C*, 2009, **29**, p 1942–1949
30. S. Kumar, T.S.N. Sankara Narayanan, S. Ganesh Sundara Raman, and S.K. Seshadri, Thermal Oxidation of Ti6Al4V Alloy: Microstructural and Electrochemical Characterization, *Mater. Chem. Phys.*, 2010, **119**, p 337–346
31. S. Kumar, T.S.N. Sankara Narayanan, S. Ganesh Sundara Raman, and S.K. Seshadri, Thermal Oxidation of CP Ti—An Electrochemical and Structural Characterization, *Mater. Charact.*, 2010, **61**, p 589–597
32. S. Kumar, T.S.N. Sankara Narayanan, S. Ganesh Sundara Raman, and S.K. Seshadri, Fretting Corrosion Behaviour of Thermally Oxidized CP-Ti in Ringer's Solution, *Corros. Sci.*, 2010, **52**, p 711–721
33. S. Kumar, T.S.N. Sankara Narayanan, S. Ganesh Sundara Raman, and S.K. Seshadri, Surface Modification of CP-Ti to Improve the Fretting Corrosion Resistance: Thermal Oxidation vs. Anodizing, *Mater. Sci. Eng. C*, 2010, **30**, p 921–927
34. D.C. Silverman, "Tutorial on Polexperttm and the Cyclic Potentiodynamic Polarization Technique," http://www.argentumsolutions.com/tutorials/polexpert_tutorialpg1.html
35. M. Jamesh, S. Kumar, and T.S.N. Sankara Narayanan, Corrosion Behavior of Commercially Pure Mg and ZM21 Mg Alloy in Ringer's Solution—Long Term Evaluation by EIS, *Corros. Sci.*, 2011, **53**, p 645–654
36. L. Peguet, B. Malki, and B. Baroux, Influence of Cold Working on the Pitting Corrosion Resistance of Stainless Steels, *Corros. Sci.*, 2007, **49**, p 1933–1948
37. F.M. Bayoumi, W.A. Ghanem, and B.G. Ateya, Electrochemical Behavior of Cr-Mo Steel Alloy in High Temperature Aqueous Sodium Chloride Solution, *Int. J. Electrochem. Sci.*, 2006, **1**, p 258–267
38. H. Guleryuz and H. Cimenoglu, Surface Modification of a Ti-6Al-4V Alloy by Thermal Oxidation, *Surf. Coat. Technol.*, 2005, **192**, p 164–170
39. A.R. Ebrahimi, F. Zarei, and R.A. Khosroshahi, Effect of Thermal Oxidation Process on Fatigue Behavior of Ti-4Al-2V Alloy, *Surf. Coat. Technol.*, 2008, **203**, p 199–203
40. K. Nakajima, K. Terao, and T. Miata, The Effect of Microstructure on Fatigue Crack Propagation of $\alpha + \beta$ Titanium Alloys: In-Situ Observation of Short Fatigue Crack Growth, *Mater. Sci. Eng. A*, 1998, **243**, p 176–181
41. J.A. Hall, Fatigue Crack Initiation in Alpha-Beta Titanium Alloys, *Int. J. Fatigue*, 1997, **19**, p 23–37
42. C. Leinenbach and D. Eifler, Influence of Oxidation Treatment on Fatigue and Fatigue-Induced Damage of Commercially Pure Titanium, *Acta Biomater.*, 2009, **5**, p 2810–2819
43. S.Y. Yu, C.W. Brodrick, M.P. Ryan, and J.R. Scully, Effects of Nb and Zr Alloying Additions on the Activation Behavior of Ti in Hydrochloric Acid, *J. Electrochem. Soc.*, 1999, **146**, p 4429–4438
44. M. Pourbaix, *Atlas of Electrochemical Equilibria in Aqueous Solutions*, Vol 1, Pergamon Press, New York, 1966, p 213
45. E. Mccafferty, *Introduction to Corrosion Science*, Springer, New York, 2010, p 212
46. E. Klar and P.K. Samal, *Powder Metallurgy Stainless Steels: Processing, Microstructures, and Properties*, ASM International, Materials Park, OH, 2007, p 155
47. D. Marecil, D. Sutiman, A. Cailean, and I. Cretescu, Effect of Vanadium Replacement by Zirconium on the Electrochemical Behavior of Ti6Al4V Alloy in Ringer's Solution, *Environ. Eng. Manage. J.*, 2008, **7**, p 701–706
48. I.C. Lavos-Valereto, S. Wolynec, I. Ramires, A.C. Guastaldi, and I. Costa, Electrochemical Impedance Spectroscopy Characterization of Passive Film Formed on Implant Ti-6Al-7Nb Alloy in Hank's Solution, *J. Mater. Sci. Mater. Med.*, 2004, **15**, p 55–59

49. S.L. Assis, S. Wolynec, and I. Costa, Corrosion Characterization of Titanium Alloys by Electrochemical Techniques, *Electrochim. Acta*, 2006, **51**, p 1815–1819
50. A. Cremasco, W.R. Osorio, C.M.A. Freire, A. Garcia, and R. Caram, Electrochemical Corrosion Behavior of a Ti-35Nb Alloy for Medical Prostheses, *Electrochim. Acta*, 2008, **53**, p 4867–4874
51. G.S. Firstov, R.G. Vitchev, H. Kumar, B. Blanpain, and J. Van Humbeeck, Surface Oxidation of NiTi Shape Memory Alloy, *Biomaterials*, 2002, **23**, p 4863–4871
52. S. Barisona, S. Cattarina, S. Daolioa, M. Musiania, and A. Tuissib, Characterization of Surface Oxidation of Nickel-Titanium Alloy by Ion-Beam and Electrochemical Techniques, *Electrochim. Acta*, 2004, **50**, p 11–18